ELSEVIER

Coordination Chemistry Reviews
198 (2000) 347–366

COORDINATION CHEMISTRY REVIEWS

www.elsevier.com/locate/ccr

# Haldane gap systems

Masahiro Yamashita *, Tomohiko Ishii, Hiroyuki Matsuzaka

*Graduate School of Science & PRESTO (JST), Tokyo Metropolitan University, 1-1 Minamiohsawa, Hachioji, Tokyo 192-0397, Japan*

Received 12 February 1999; received in revised form 1 June 1999; accepted 21 July 1999

**Contents**



**Abstract**

Haldane gap compounds with $S=1$ formulated as $[Ni(AA)_2X]Y$ ($(AA)_2$ = (diamines)$_2$, linear-tetramines, $N_4$-macrocycles; $X=NO_2$ and $N_3$; $Y=ClO_4$, $BF_4$ and $PF_6$) and $(CH_3)_4N[Ni(NO_2)_3]$, and with $S=2$ formulated as $[Mn(AA)_2Cl_3]$ (AA = bipy and phen) are

* Corresponding author. Tel.: +81-426-77-2550; fax: +81-426-77-2525.
*E-mail address:* yamashit@comp.metro-u.ac.jp (M. Yamashita)


PII: S0010-8545(99)00212-X

described. They have one-dimensional structures with bridging ligands. The Haldane conjecture was proven by magnetic susceptibility and high-field magnetization measurements. The magnitudes of the Haldane gap with $S=1$ can be controlled by combination of the bridging ligands, in-plane ligands, and counteranions as follows: X, $N_3 > NO_2$; AA, en $\geqq$ tn > linear-tetramines > dmpn > $Me_6$[14]ane$N_4 \geqq$ [15]ane$N_4$; Y, $ClO_4 > PF_6$. In spite of a similar structure to Haldane gap compounds, the [Ni([15]ane$N_4$)$N_3$]$PF_6$ and [Ni(en)$_2$($NO_2$)]$BF_4$ species show spin-glass behavior, which is very novel in one-dimensional spin systems. The [Mn(bipy)$Cl_3$] is regarded as the first example of the Haldane gap system with $S=2$. 

*Keywords:* Haldane gap; One-dimensional Heisenberg antiferromagnet; One-dimensional $Ni^{2+}$ compounds; One-dimensional $Mn^{3+}$ compounds

## 1. Introduction

Low-dimensional magnetic systems are of current interest because they show peculiar quantum effects [1]. A one-dimensional Heisenberg antiferromagnet (1D-HAF) is expressed by the following simple spin Hamiltonian;

$$H = -J\Sigma S_i S_{i+1} \quad (1)$$

where $J$ is the intrachain coupling constant. Then, $J<0$ and $J>0$ show antiferromagnetic and ferromagnetic interactions, respectively. The eigenstates of Eq. (1) were given by the Bethe ansatz in the case of $S=1/2$ [2]. Hulthen used them to obtain the exact values for the ground state energy of an $S=1/2$ linear chain Heisenberg antiferromagnet [3]. Yang and Yang exactly proved the Bethe ansatz for the ground state of a finite chain [4]. Magnetization at zero temperature was calculated by Griffiths [5]. Bonner and Fisher carried out numerical calculations for several different spins up to $N=11$ and estimated the thermal and magnetic properties of an infinite chain by extrapolation [6]. They showed that the energy level of the spin chain system is gapless and no long range ordering occurs down to $T=0$ K. The low-lying excited states are explained by the spin wave theories proposed by Anderson [7] and Kubo [8] in 1952, and later calculated exactly for an $S=1/2$ infinite chain by de Cloizeaux and Pearson [9]. In spite of this extensive work, studies of $S \geqq 1$ were rarely carried out because of difficulties in the calculations and it was believed that the physical properties are independent with respect to the spin quantum numbers until Haldane's conjecture was proposed.

In 1983, Haldane predicted [10] that a 1D-HAF should have an energy gap between the singlet ground state and the first excited triplet states in the case of an integer spin quantum number, while the energy levels are gapless in the case of a half integer spin quantum number, as shown in Fig. 1. Therefore, the magnetic susceptibility approaches zero at $T=0$ in the Haldane gap system, while the magnetic susceptibility decreases to finite values in the case of the half-integer spin. In the high-field magnetization measurements, with an increase in magnetic field, a component of the first triplet excited states decreases in energy and crosses the

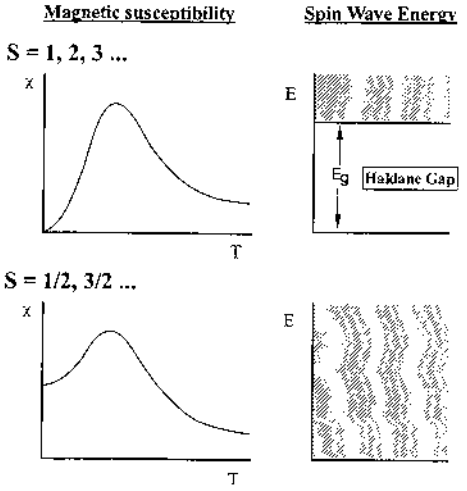


Fig. 1. Magnetic susceptibilities and spin wave energy in case of integer spin quantum number (top) and half-integer spin quantum number (bottom).

ground state, where the magnetic susceptibility appears at a higher magnetic field than the critical magnetic field ($H_c$) as shown in Fig. 2. Since Haldane's conjecture appeared, many theoretical and experimental studies have been carried out to verify it. Most have accepted Haldane's conjecture. Some calculations give the correlation of $E_g \sim 0.41|J|$ by Monte Calro methods [11,12].

The first Haldane gap compound was $[Ni(en)_2(NO_2)]ClO_4$, which was synthesized in 1981 by Meyer et al. [13] and first recognized as a Haldane gap compound by Renard et al. in 1987 [14]. So far several Haldane gap compounds with $S = 1$ and only one compound with $S = 2$ have been synthesized [15]. In this review, we will survey the Haldane gap compounds with $S = 1$ and $S = 2$, along with novel spin-glass compounds having similar structures. We will especially describe the magnetic properties of the Haldane gap system mainly from the view point of the correlation between the Haldane gap $E_g$ and the antiferromagnetic interaction $J$.

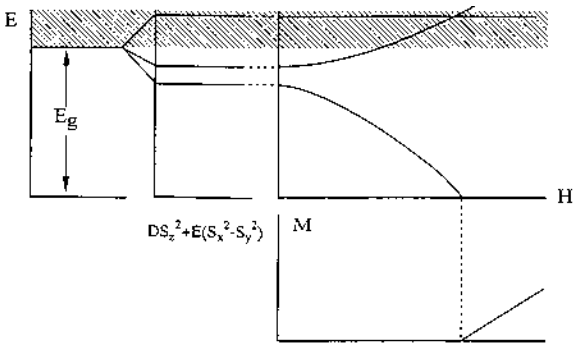


Fig. 2. Energy diagram and magnetization under inducing magnetic field.

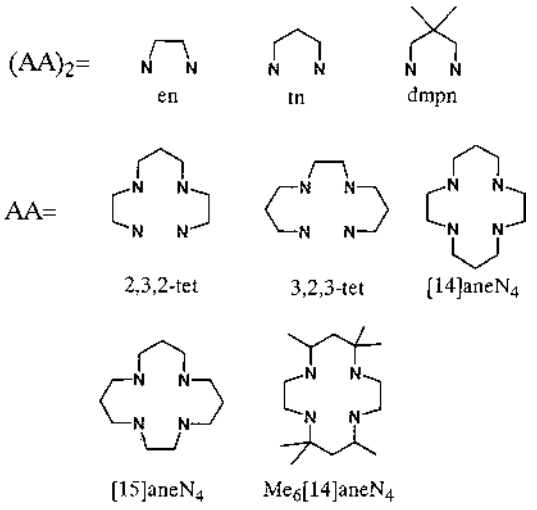


Fig. 3. In-plane ligands and their abbreviations.

## 2. Compounds with $S = 1$

A series of one-dimensional $Ni^{2+}$ compounds, $[Ni(AA)_2X]Y$ ($(AA)_2$ = (diamines)$_2$, linear-tetramines, $N_4$-macrocycles; X = $NO_2$ and $N_3$; Y = $ClO_4$, $PF_6$, $BF_4$ etc.) and $(CH_3)_4N[Ni(NO_2)_3]$, have been synthesized. In-plane ligands and their abbreviations are shown in Fig. 3.

### *2.1. Haldane gap compounds*

#### *2.1.1. $[Ni(en)_2(NO_2)]ClO_4$ (NENP)*

The first Haldane gap compound $[Ni(en)_2(NO_2)]ClO_4$ [13,14], is usually abbreviated as NENP. The one-dimensional structure is shown in Fig. 4. This compound has orthorhombic symmetry with lattice constants of $a = 15.223$, $b = 10.300$ and $c = 8.293$ Å. The $Ni^{2+}$ ion is octahedrally coordinated with equatorial $N_4$ atoms of two ethylenediamines. Each $Ni^{2+}$ ion is bridged with the nitrite group ($NO_2$) bounded on one side by an N atom and the other side by an O atom, where the Ni–N (axial) and Ni–O distances are 2.163 and 2.183 Å, respectively. The chain is parallel to the $b$-axis.

The magnetic susceptibility shows a broad maximum at about 60 K, as shown in Fig. 5, which is characteristic of 1D-HAF [14]. As the temperature decreases further, the magnetic susceptibility abruptly decreases to zero. This behavior ($T < 5$ K) is ascribed to the existence of the Haldane gap, given by the following relation;

$$\chi(T) = \chi(0) + C \exp(-E_g/k_BT)$$

with $E_g = 11$ and 17 K for respective field directions parallel and perpendicular to the chain axis. In the higher temperature region, the data are fitted by the

theoretical curve with $J = -47.5$ K [13]. Particularly, the susceptibility curves reveal no transition to three-dimensional long-range ordering (3D-LRO) within the temperature range down to $T = 1.5$ K, which implies that the electron spin relaxes to the non-magnetic ground state. A direct observation of the Haldane gap was obtained by the inelastic neutron scattering measurement [14,16].

Katsumata et al. have performed high field magnetization measurements and obtained clear evidence for the existence of the Haldane gap [17]. The magnetiza-

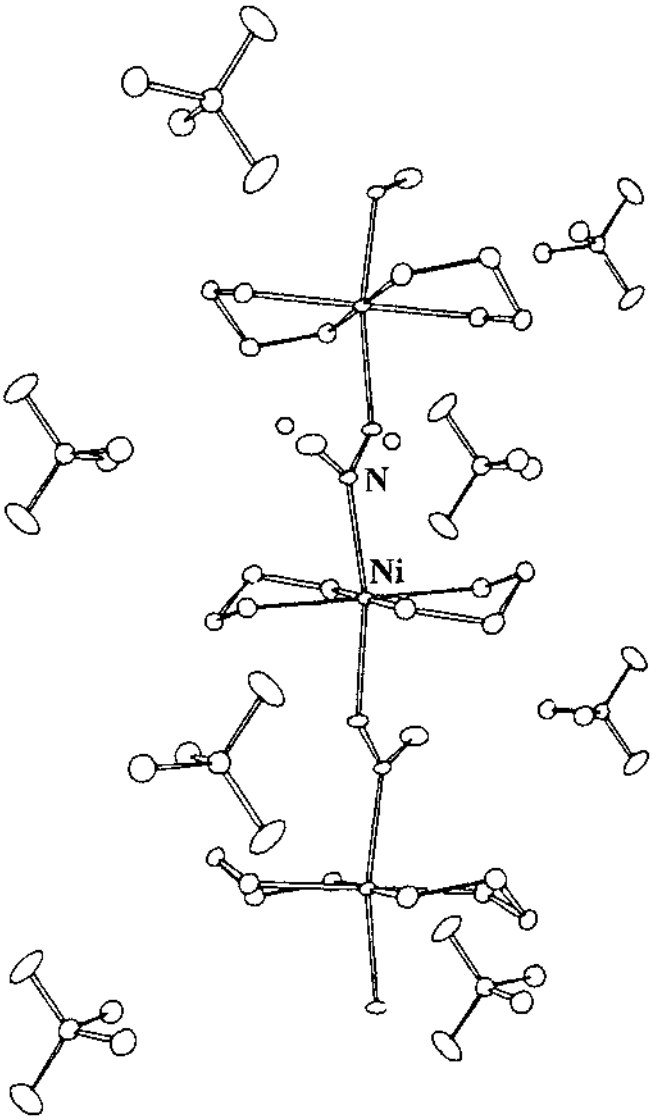


Fig. 4. Crystal structure of $[Ni(en)_2(NO_2)]ClO_4$.

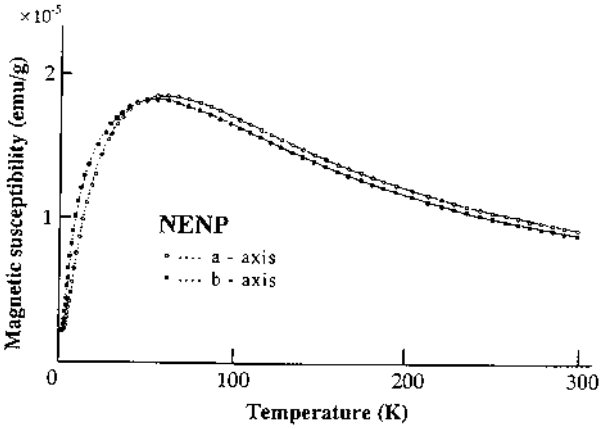


Fig. 5. Magnetic susceptibilities of $[Ni(en)_2(NO_2)]ClO_4$.

tion is very small in the low field region and begins to increase sharply at finite field $H \| c = 8$ T and $H \perp c = 12$ T for the parallel and perpendicular directions with respect to the chain axis as shown in Fig. 6.

### 2.1.2. $[Ni(tn)_2(NO_2)]ClO_4$ (NINO)

NINO has a similar crystallographic structure to NENP, with lattice constants of $a = 15.378$, $b = 10.575$, and $c = 8.485$ Å and space group of $Pbn2_1$. The Ni–N (axial) and Ni–O distances are 2.152 and 2.282 Å, respectively [18]. The magnetic susceptibility shows a broad peak around 60 K and exponentially decreases at very low temperature. The least-squares fitting of the experimental data to the theoretical calculation leads to $E_g = 14.2$ K, $J = -49.9$ K, $g_a = 2.23$, $g_b = 2.17$ and $g_c = 2.22$ [19,20].

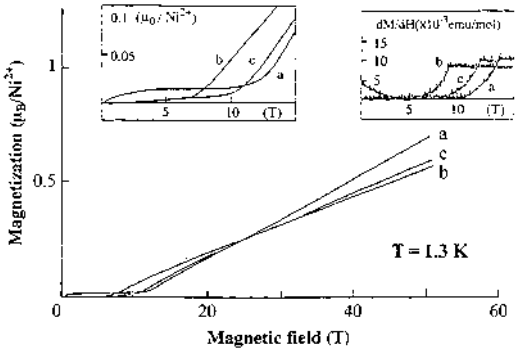


Fig. 6. Field-induced magnetization curves of single crystal of $[Ni(en)_2(NO_2)]ClO_4$.

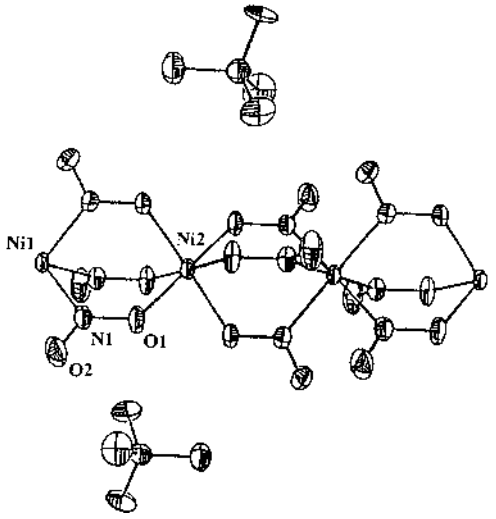


Fig. 7. Crystal structure of $(CH_3)_4N[Ni(NO_2)_3]$.

*2.1.3. $[Ni(dmpn)_2NO_2]PF_6 \cdot H_2O$*

The magnetic susceptibilities show a broad maximum around 10 K and abruptly decrease with decrease of temperature, indicating the existence of a Haldane gap. The $g$ and $J$ are estimated at 2.16 and $-9.0$ K, respectively, while the low temperature component, $E_g$ is estimated at 3.6 K [21]. The $E_g$ and $lJl$ values of this compound are remarkably small compared with those of the $NO_2$-bridged compounds NENP and NINO.

*2.1.4. $(CH_3)_4N[Ni(NO_2)_3]$ (TMNIN)*

The $(CH_3)_4N[Ni(NO_2)_3]$ (TMNIN) is a chain-like structure coupled via three $NO_2$ anions. The structure consists of infinite chains of $Ni^{2+}$ ions with adjacent Ni ions bridged by three *cis*-É-nitrite ligands such that alternative Ni ions are chemically distinct, with Ni(1) octahedrally coordinated with six nitrite nitrogens and Ni(2) octahedrally coordinated with six nitrite oxygens. The $(CH_3)_4N$ cations are located in positions along the 3-fold rotation axes and form a channel that separates the Ni chains. The intrachain Ni–Ni distance is 3.541 Å, and the interchain separation is 9.1029 Å (Fig. 7). The magnetic susceptibility in the high temperature region is consistent with one-dimensional antiferromagnetism with $J = -12$ K and $g = 2.25$. Below 10 K, a strong decrease in the susceptibility and proton relaxation rate is observed, in agreement with the Haldane prediction of a singlet ground state for $S = 1$, one-dimensional Heisenberg antiferromagnet. From the magnetization versus field data at low temperature, the Haldane gap is estimated at 4.5 K, close to the expected value $0.41lJl$ for the $S = 1$, one-dimensional Heisenberg antiferromagnet [22,23]. The heat capacity of the polycrystalline TMNIN was measured. The result was qualitatively the same as NENP, where no 3D-LRO is observed [24].

*2.1.5. $[Ni(tn)_2N_3]ClO_4$ (NINAZ)*

NINAZ crystallizes in the orthorhombic system with the lattice constants $a = 15.384$, $b = 10.590$, and $c = 8.507$ Å. The chain consists of linear chain $Ni^{2+}$ ions which are bridged by $N_3$ bridging group along the $c$-axis. These chains are well separated from each other by $ClO_4$ ions. The Ni–Ni distance along the chain is 5.849 Å.

The magnetic susceptibility of a single crystal sample of NINAZ exhibits a broad maximum at about 150 K, indicating the stronger antiferromagnetic coupling in the chain compared with those of the $NO_2^-$ bridged compounds. The magnetic susceptibility shows an exponential decrease at low temperature, reflecting a clear manifestation of the Haldane gap. The high temperature data can be fitted by the theoretical curve with $J = -144$ K. From the low temperature component, the $E_g$ is estimated at about 41 K. These are the highest values observed in the Haldane gap system and are related to a strong one-dimensional antiferromagnetic interaction. They are the same as data reported for the powdered sample as $J = -120$ K and $E_g = 40$ K [25,26].

*2.1.6. $[Ni(dmpn)_2N_3]ClO_4$ (NDMAZ)*

NDMAZ crystallizes in the monoclinic space group $C2$ and the lattice constants are $a = 18.869$, $b = 8.152$, $c = 6.098$ Å, and $\beta = 98.27°$. The structure consists of $Ni^{2+}$ chains along the crystal $c$-axis; each $Ni^{2+}$ ion is bridged by $N^{3-}$ as shown in Fig. 8. Two dmpn ligands are coordinated to each $Ni^{2+}$ ion. The Ni–N (axial) and

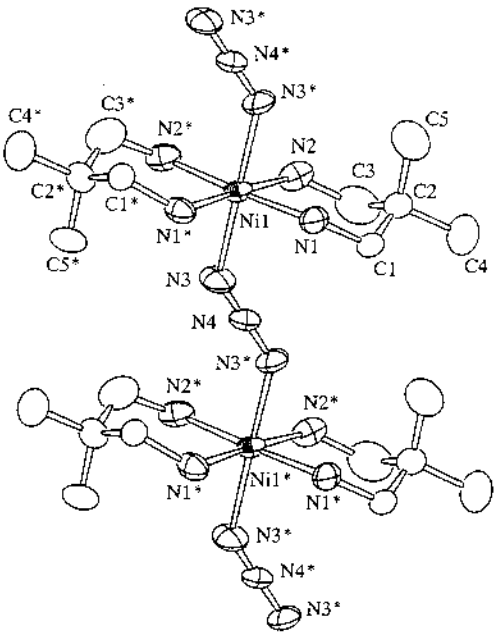


Fig. 8. Crystal structure of $[Ni(dmpn)_2N_3]ClO_4$.

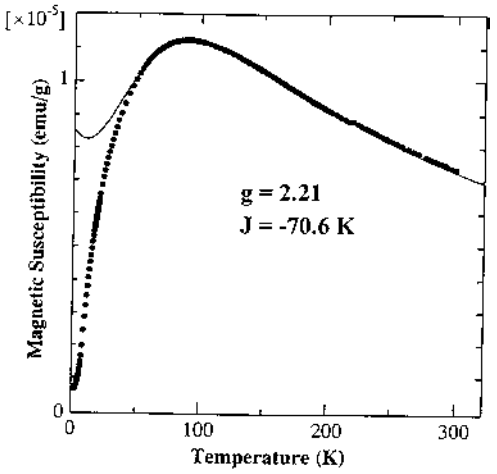


Fig. 9. Magnetic susceptibilities of $[Ni(dmpn)_2N_3]ClO_4$.

Ni–N (equatorial) distances are 2.101 and 2.111 Å, respectively. All $Ni^{2+}$ sites are crystallographycally equivalent, while NENP has two inequivalent $Ni^{2+}$ sites due to the bridging $NO_2^-$ as shown previously [27].

The magnetic susceptibility of polycrystalline samples of NDMAZ show a broad peak at around 90 K which exponentially decreases with lower temperature (Fig. 9). A discontinuity of the magnetic susceptibility related to a phase transition is observed around 230–240 K, suggesting the co-existence of two kinds of antiferromagnetic interaction $J_1$ and $J_2$ for the high and low temperature region, respectively. The data were fitted to the theoretically calculated one with the parameters $g = 2.12$ and $J_2 = -70.6$ K. From the low-temperature components, the Haldane gap due to $J_2$ for the low temperature region is estimated to be 22 K. Takeuchi et al. also performed a high-field magnetization process under a magnetic field up to 30 T. The field dependence of magnetization shows that the critical field $H_c$ is around 14 T (Fig. 10) [28].

The main difference between NENP and NDMAZ is the direction of the magnetic $g$-tensor, that is, alternatively tilted and parallel, respectively (Fig. 11). Accordingly 3D-LRO is expected in NDMAZ at low temperature and under a high magnetic field. Katsumata et al. performed a heat capacity ($C_p$) measurement on a single crystal of NDMAZ under high magnetic fields and at low temperatures as shown in Fig. 12. A $C_p$ anomaly was observed at about 9 K and at 12 T. They interpreted this anomaly as an indication of field induced long-range magnetic ordering, which is the first observation in Haldane gap systems [29].

The pressure effect on Haldane gap compounds is very interesting. Two possibilities which are contrary to each other are assumed. One is an increase in the Haldane gap due to an increase in the orbital overlap between the $Ni^{2+}$ ions and the bridging ligands. The other is a decrease in the Haldane gap due to the lowering of the first excited triplet state. In order to clarify the pressure effect, the tempera-

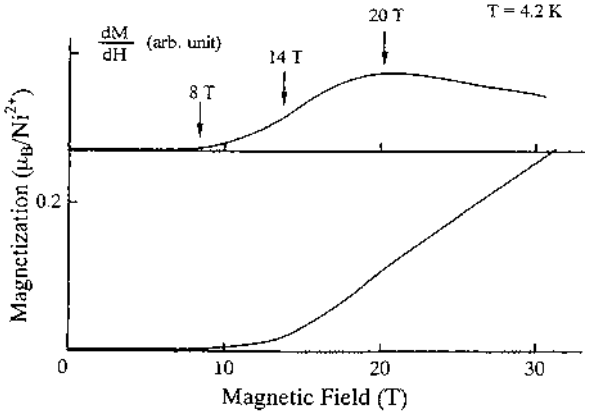


Fig. 10. Field-induced magnetization curve of $[Ni(dmpn)_2N_3]ClO_4$.

ture-dependent magnetic susceptibilities of polycrystalline NDMAZ were measured under pressure up to 10 kbar [30] (Fig. 13). With increase of pressure, the absolute value of the magnetic susceptibility decreases. At the same time, the peaks gradually shift to higher temperatures. Accordingly, the experimental data were fitted to Meyer's equations. Then, the *lJl* values under pressure are obtained as shown in Fig. 14. With an increase in pressure, the *lJl* values increase by 50%. This is due to an increase in the orbital overlap between $Ni^{2+}$ and the $N_3$-bridging ligands under pressure.

### *2.1.7. $[Ni(dmpn)_2N_3]PF_6$*

The synthesis and structural determination were carried out by Monfort et al. The compound crystallizes in the orthorhombic system of space group *Pnmn* with lattice constants of $a = 18.046$, $b = 8.705$ and $c = 6.139$ Å. The chain runs along the *c*-axis. The Ni–N distances in the axial and equatorial positions are 2.125 and 2.108 Å, respectively [31].

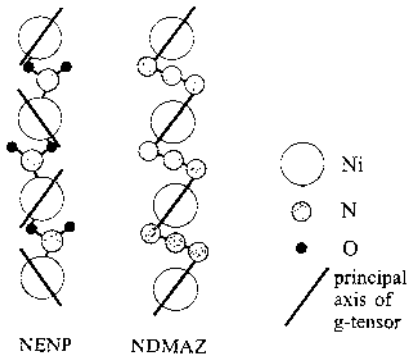


Fig. 11. Direction of the principle axis of g-tensor of NENP (left) and NDMAZ (right).

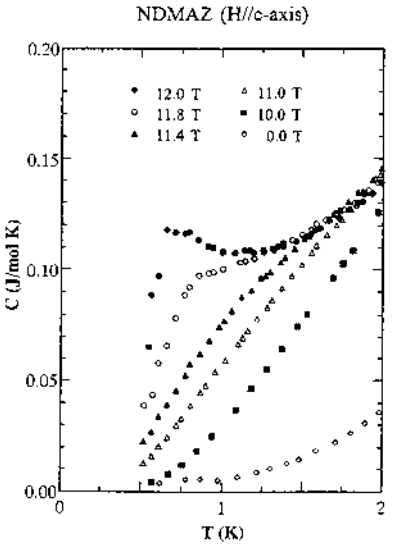


Fig. 12. Heat capacity of single crystal of $[Ni(dmpn)_2N_3]ClO_4$.

The magnetic susceptibility of a single crystal of this compound was measured. A broad peak appears at about 30 K and the susceptibilities decrease steeply for all of the crystal axes when the temperature is decreased further. There is an anisotropy

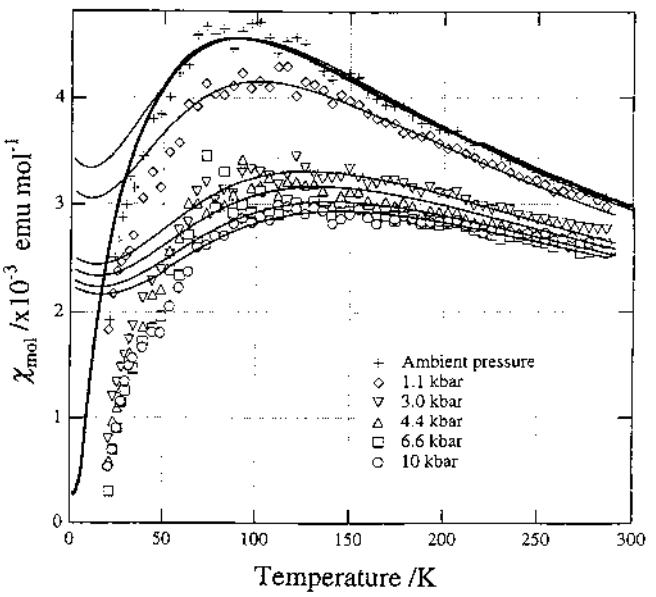


Fig. 13. Pressure effect of temperature-dependent magnetic susceptibilities of $[Ni(dmpn)_2N_3]ClO_4$.

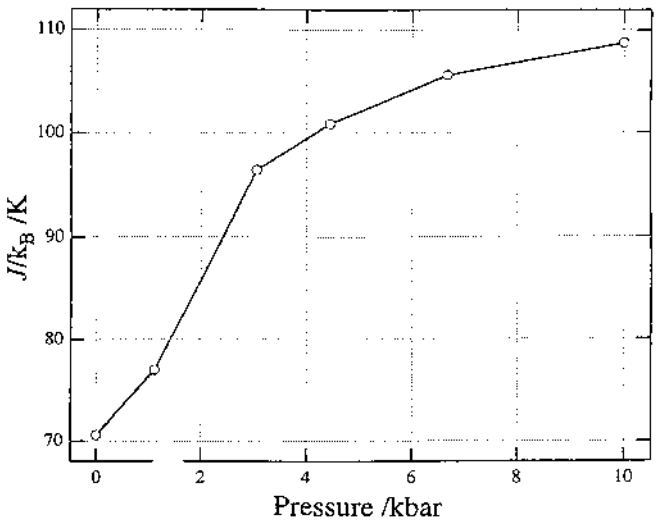


Fig. 14. $J$ values under pressure up to 10 kbar.

in the magnetic susceptibility which can be explained as due to the single-ion anisotropy of $Ni^{2+}$ such as NENP and NDMAZ. The $g$ and $E_g$ are estimated at 2.15 and 5.0 K, respectively. The value of $J$ in this compound is almost half of that in NDMAZ [31]. The heat capacity of a single crystal of this compound was measured. With increasing field, an anomaly was clearly observed. This is due to 3D-LRO similar to the NDMAZ [32].

### *2.1.8. [Ni(3,2,3-tet)$N_3$]$ClO_4$*

The synthesis and single-crystal structural determination were carried out by Escuer et al. The complex crystallizes in the orthorhombic system, space group *Pbca* with $a = 17.151$, $b = 16.267$ and $c = 11.478$ Å. In this compound, each $Ni^{2+}$ ion was placed in an octahedral environment with μ-azido group in the *trans* form. The chains were parallel to the $c$-axis and were well separated by $ClO_4$ ions. The Ni–N (axial) and Ni–N(equatorial) distances were 2.181 and 2.103 Å, respectively [33].

Magnetic susceptibility measurements were carried out by Takeuchi et al. and the $J$ and $g$ values estimated at $-90.2$ K and 2.38, respectively. The high-field magnetization measurements were carried out along three crystalline principal axes, $a$, $b$ and $c$ at 4.2 K. The qualitative behavior was almost the same for NENP and NDMAZ. The Haldane gap was estimated at 25.3 K [33].

### *2.1.9. [Ni($Me_6$[14]ane$N_4$)$N_3$]$ClO_4$*

The synthesis and structure determination were carried out by Escuer et al. The compound crystallized in the orthorhombic system with space group *Pnab* of lattice constants of $a = 12.134$, $b = 16.107$ and $c = 34.527$ Å. The Ni–N(axial) distance was 2.179 Å. The chain was parallel to the $c$-axis [34].

The magnetic susceptibilities show a broad peak around 70 K which decrease abruptly with any decrease in temperature. The $g$ and $J$ were estimated at 2.11 and $-57.3$ K. From the low temperature components, $E_g$ was estimated at 12.9 K [35].

#### 2.1.10. [Ni([15]aneN$_4$)N$_3$]ClO$_4$

Magnetic susceptibilities showed a broad peak around 60 K and then decreased abruptly with decreasing temperature. The $g$ and $J$ were estimated at 2.07 and $-51.8$ K, respectively, while the $E_g$ was estimated at 13 K [35].

### 2.2. Control of the magnitudes of Haldane gaps

The magnitudes of Haldane gaps and $J$ values were obtained in the compounds, [Ni(AA)$_2$X]Y and TMNIN. In the case of TMNIN, there are three $NO_2$ bridging ligands between two adjacent Ni metals. For this reason we cannot directly compare the $J$ value of TMNIN with those of the other $NO_2$-bridged compounds. We summarize the $J$ and $E_g$ values of these compounds in Table 1, and also plot them in Fig. 15 [36]. The straight line is the theoretical correlation between $E_g$ and $|J|$ obtained by the Monte Carlo calculation method, $E_g \sim 0.41|J|$. Most experimental data fall below the line. The effect of the bridging ligands, the in-plane ligands, and the counteranions on the Haldane gaps is as follows; X, $N_3 > NO_2$; AA, en $\geqq$ tn > linear-tetramine > dmpn > Me$_6$[14]aneN$_4$ $\geqq$ [15]aneN$_4$; Y, $ClO_4 > PF_6$. The effect of the bridging ligands follows from the different strengths of the coordination abilities. The in-plane ligands and counteranions are considered to affect the Haldane gap by their difference in bulkiness. From these results, we can control the magnitude of the Haldane gap by substituting the bridging ligands, the in-plane ligands, and the counteranions, especially in the case of selecting the $N_3$ molecule as the bridging ligand. Escure et al. described the mechanism for changing the $J$ values with three factors; N–N–N angle, Ni–$N_3$–Ni torsion angle and Ni–N distances [31,33,34]. The in-plane ligands and the counteranion play a role as a spacer modifying the three parameters in the $N_3$-bridging system.

Regarding the effect of the bridging ligands, a comparison between $N_3^-$ and $NO_2^-$ relates the magnitude of the $J$ and the structural parameters for these two bridges [13,33]. Among $NO_2$-bridging system, the $J$ value tends least to be changed and is almost constant independent of the bond parameters, comparing between NENP and NINO [13,37], in spite of the compounds with different in-plane ligands.

### 2.3. Other Haldane gap compounds

Four other compounds are regarded as Haldane gap compounds. The NiC$_2$O$_4$·2L ($C_2O_4^{2-}$ = oxalate; L = 2-methylimidazole = MIz and 1,2-dimethylimidazole = DMIz) were synthesized [38]. They have a one-dimensional structure with octahedral $Ni^{2+}$ atoms bridged by $C_2O_4^{2-}$ and coordinated by two L in axial positions. From their magnetic susceptibilities $J$ and $E_g$ are obtained as $-35.7$ and 20.3 K for L = MIz, and $-34.6$ and 19.0 K for L = DMIz. High-field magnetization measure-

ments were performed on powder samples of these compounds up to 36 T. The observed magnetizations are very small below the definite critical field $H_c$ near 13 T and increase abruptly above $H_c$, indicating clear evidence of the existence of the non-magnetic ground and magnetic excited state.

The $E_g$ and $J$ of $AgVP_2S_6$ are estimated at 320 and $-400$ K, respectively [39]. The $E_g$ and $J$ of $Y_2BaNiO_5$ are estimated at 100 and $-285$ K, respectively [40].

Table 1
The magnitudes of Haldane gaps $E_g$ and the antiferromagnetic interaction $J$ values in the compounds $[Ni(AA)_2X]Y$ and TMNIN, (a) $N_3$-bridged and (b) $NO_2$-bridged

| In-plane ligand (X) | | Counter anion (Y) | |
|---|---|---|---|
| | | $ClO_4$ | $PF_6$ |
| (*a*) *$N_3$-bridged* | | | |
| tn | $J$ | $-144$ K, $-120$ K [25,26] (NINAZ) | $-70.6$, $-55.8$ cm$^{-1}$ [31] |
| | $E_g$ | 41 K, 40 K [25,26] | |
| dmpn | $J$ | $-70.6$ K, $-101.4$ cm$^{-1}$ [34](NDMAZ) | $-30$ K, $-41.1$, $-19.4$ cm$^{-1}$ [31] |
| | $E_g$ | 21.6 K | |
| 232-tet | $J$ | $-37$ K ($-26.9$ cm$^{-1}$) | |
| | $E_g$ | | |
| 323-tet | $J$ | $-90.3$ K [33] ($-62.7$ cm$^{-1}$) | |
| | $E_g$ | 25.3 K | |
| 333-tet | $J$ | $-116$ K ($-80.7$ cm$^{-1}$), $-37.4$ cm$^{-1}$ | $-26.6$ K ($-18.5$ cm$^{-1}$) |
| | $E_g$ | | |
| $[14]aneN_4$ | $J$ | $-56$ K ($-39.2$ cm$^{-1}$) | |
| | $E_g$ | | |
| $Me_6[14]aneN_4$ | $J$ | $-41.1$, $-36.4$ cm$^{-1}$ [34] $-57.3$ K [35] | |
| | $E_g$ | 12.9 K [35] | |
| $[15]aneN_4$ | $J$ | $-51.8$ K [35] | |
| | $E_g$ | 13.0 K [35] | |
| (*b*) *$NO_2$-bridged* | | | |
| en | $J$ | $-47.5$ K [13] ($-33$ cm$^{-1}$) (NENP) | |
| | $E_g$ | 17.0 K [13] | |
| tn | $J$ | $-49.9$ K [19,20] (NINO) | |
| | $E_g$ | 14.2 K [19,20] | |
| dmpn | $J$ | | $-9.0$ K [21] |
| | $E_g$ | | 3.6 K [21] |
| 333-tet | $J$ | $-43.5$ K | |
| | $E_g$ | 10.6 K | |
| | | *Counter cation* ($(CH_3)_4N$) | |
| $(CH_3)_4$-N[$Ni(NO_2)_3$] | $J$ | $-12$ K [22,23] (TMNIN) | |
| | $E_g$ | 4.5 K [22,23] | |

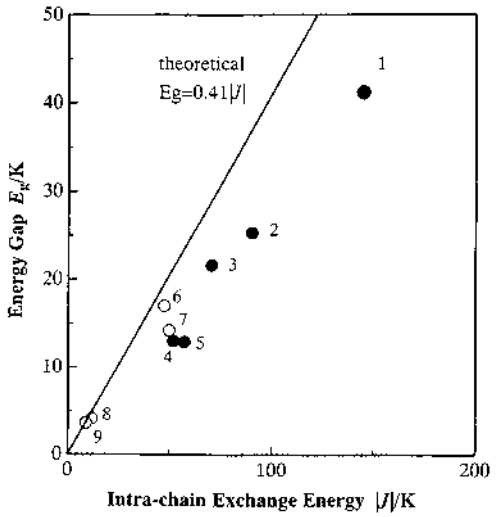


Fig. 15. Relation between $E_g$ and $|J|$. 1; $[Ni(tn)_2N_3]ClO_4$, 2; $[Ni(3,2,3\text{-tet})N_3]ClO_4$, 3; $[Ni(dmpn)_2N_3]ClO_4$, 4; $[Ni([15]aneN_4)N_3]ClO_4$, 5; $[Ni(Me_6[14]aneN_4)N_3]ClO_4$, 6; $[Ni(en)_2(NO_2)]ClO_4$, 7; $[Ni(tn)_2(NO_2)]ClO_4$, 8; $(CH_3)_4N[Ni(NO_2)_3]$, 9; $[Ni(dmpn)_2(NO_2)]PF_6 \cdot H_2O$.

### 2.4. Spin-glass behaviors

A DC magnetic susceptibility of a single crystal of $[Ni([15]aneN_4)N_3]PF_6$ was measured. Two modes of measurements were performed: zero field cooled measurement (ZFC) and field cooled measurements (FC). In the ZFC measurement, the sample was cooled from high temperature to 1.8 K in zero magnetic field, then a field of 100 G was applied and the magnetic susceptibilities were measured with increasing temperature. In the FC case, however, the measurement was performed under the applied field with decreasing temperature from room temperature. The results are shown in Fig. 16. The DC susceptibilities of this compound differ very much from that of the typical $S = 1$ Haldane gap compounds, e.g. NENP and NDMAZ. No rounded maximum is found in this compound. Instead, for both ZFC and FC measurements, the susceptibilities of this compound steadily increase from room temperature down to about 30 K and then drastically increase from 30 to about 20 K. Thereafter, the susceptibilities for the ZFC measurement decrease greatly, while that for the FC measurement remains almost constant with decreasing temperature [41].

An AC susceptibility measurement was carried out (Fig. 17). A cusp was observed in the temperature dependence, the position of which shifts to the high temperature side with increasing frequency. The temperature corresponding to the cusp at the lowest frequency (0.1 Hz) is about 22 K, which is slightly larger than that for the DC measurement (20 K). This is reasonable because the DC measurement is a specific case of an AC measurement in zero frequency limit.

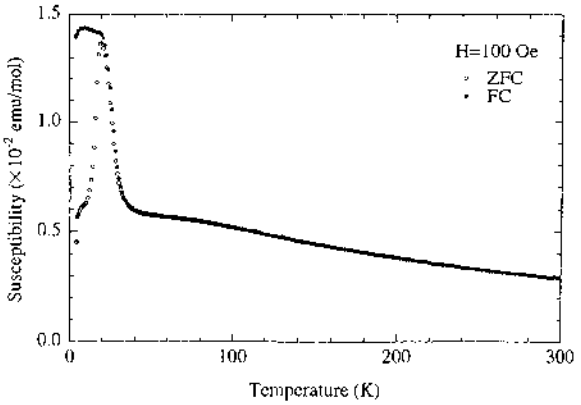


Fig. 16. Zero field cooled (ZFC) and field cooled (FC) measurements of DC magnetic susceptibilities of $[Ni([15]aneN_4)N_3]PF_6$.

The behavior of both these DC and AC susceptibility measurements is typical of a spin-glass compound. This compound also shows hysteresis under magnetization, due to a weak ferromagnetic interaction. Therefore, this compound is called a 'correlated spin-glass' (Fig. 18).

This compound crystallizes in the orthorhombic system with space group $P2nn$ and unit-cell parameters of $a = 11.322$, $b = 13.862$ and $c = 6.173$ Å. The crystal consists of two sets of linear chains (one through the vertices and the other through the body-center of the unit-cell) on which Ni ions and azido groups alternate following the sequence $-Ni^{2+}-N_3-Ni^{2+}-N_3-$ in the $c$-axis. The $PF_6^-$ ions are accommodated in the big vacancies between each chain. In the chain, a $Ni^{2+}$ ion is surrounded pseudo-octahedrally by four nitrogen atoms of the in-plane ligand and two from the azido group. In spite of the $[15]aneN_4$ ligand, the resolved structure shows the $[16]aneN_4$ ligand. This is due to the rotational disorder of the

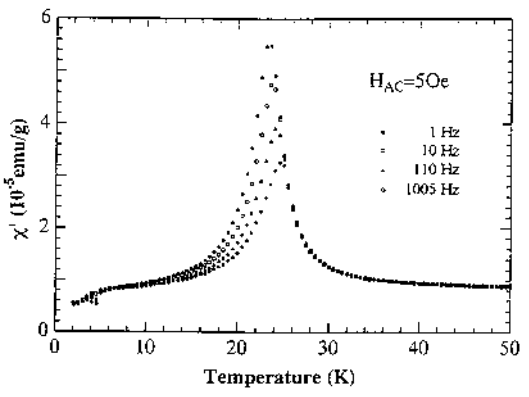


Fig. 17. AC susceptibilities of $[Ni([15]aneN_4)N_3]PF_6$.

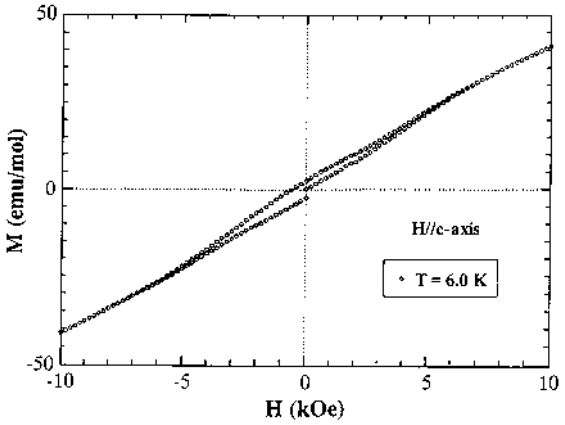


Fig. 18. Hysteresis curve under magnetization of $[Ni([15]aneN_4)N_3]PF_6$.

$[15]aneN_4$ ligand. Such a phenomenon is usually observed in the $[15]aneN_4$ ligand. From the Weissenberg X-ray oscillation with the oscillation axis parallel to *c*-axis and also, from the powder pattern, a superlattice along the *c*-axis was found, which is about twice the *c*-axis. This indicates that the packing sequence of the in-plane ligands along the chain is -1-2-1-2- in the 'actual' crystal instead of -5-5-5-5- in the

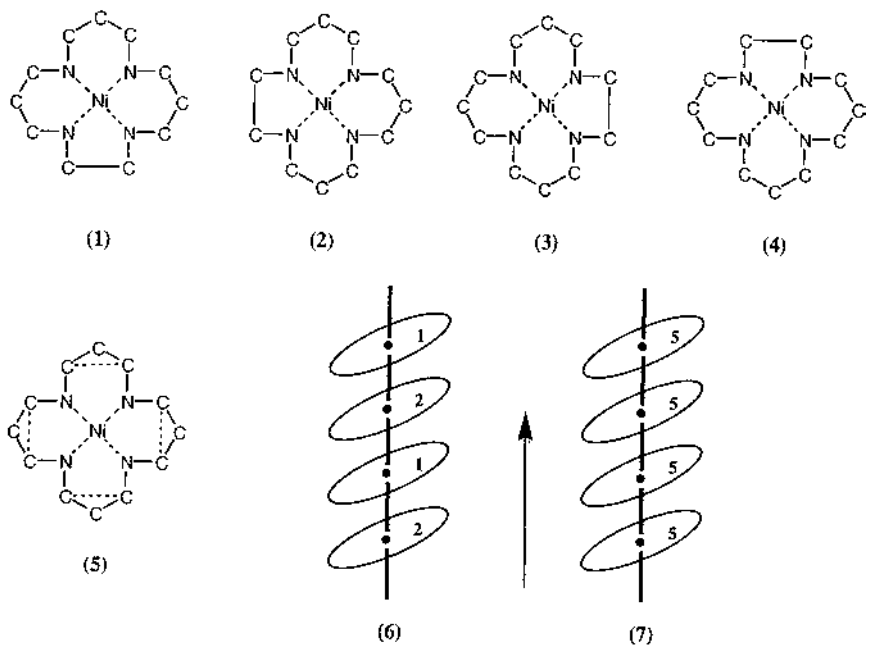


Fig. 19. Diagrammatic configuration of the in-plane ligands in 'actual' (1–4) and 'ideal' (5) crystal and their packing modes along the chain direction in 'actual' (6) and 'ideal' (7) crystal.

'ideal' crystal as shown in Fig. 19. For the same Weissenberg X-ray film, the diffraction spots corresponding to the superlattice are broad compared to those corresponding to the normal lattice. This is reasonable if it is assumed that a small part of the in-plane ligands do not pack in a well-ordered -1-2-1-2- sequence in the 'actual' crystal. This disorder in the packing sequence of the in-plane ligands will result in a broadening of the superlattice diffraction spots. Such disorder may lead these compounds to have a spin-glass behavior. Similar spin-glass behavior is also observed in $[Ni(en)_2(NO_2)]BF_4$.

## 3. Compounds with $S = 2$

### *3.1. [Mn(bipy)$Cl_3$]*

From numerical calculations, $E_g/|J|$ is predicted to be very small for $S = 2$. Therefore, it is very difficult to find Haldane gap compounds with $S = 2$.

The first Haldane gap compound with $S = 2$, $[Mn(bipy)Cl_3]$ (bipy = 2,2'-bipyridine) was discovered by Granroth [15]. The magnetic properties of these compounds were first reported by Goodwin and Sylva down to 118 K in 1967 [42]. The crystal structure was reported by Perlepes et al. in 1991 [43]. The system consists of a quasi-linear chain of $Mn^{3+}$ ($S = 2$) ions in $Mn(bipy)Cl_2$ units, asymmetrically connected by bridging $Cl^-$ ions. The $Mn^{3+}$ coordination is a distorted octahedron where the Mn–Cl bond along the chain axis (MnCl(1) = 2.51 and Mn–Cl(1') = 2.71 Å) are longer than those in the equatorial plane (2.24 Å). Axial elongation results in singly occupied $dz^2$ orbital and a value of $D < 0$. The Mn–Mn intrachain distance is 4.83 Å, and the strongest Mn–Mn interaction is through overlap of the metal $dz^2$ orbitals with the chlorine bridge. The Mn–Cl–Mn angle of 135° is consistent with the antiferromagnetic exchange.

The magnetic susceptibilities of this compound were measured from 1.8 to 300 K with magnetic field parallel and perpendicular to the chains yielding $g = 2$ and $J = -35$ K. The magnetization $M$ was studied at 30 mK and 1.4 K in a magnetic field up to 16 T. No evidence of long-range order is observed. Depending on the crystal orientation, $M = 0$ at 30 mK until a critical field is achieved ($H \| c = 1.2 \pm 0.2$ T and $H \perp c = 1.8 \pm 0.2$ T), where $M$ increases continuously as $H$ is increased. These results are interpreted as evidence of a Haldane gap.

### *3.2. [Mn(phen)$Cl_3$]*

$[Mn(phen)Cl_3]$ (phen = phenanthroline) was synthesized by Yamashita et al. [44]. The crystal structure is essentially the same as that of $[Mn(bipy)Cl_3]$. The Mn–Cl distances in equatorial and axial positions are 2.228 and 2.638 Å, respectively and the Mn–Cl–Mn angle is 134.6 K.

However, in spite of the similar structure to $[Mn(bipy)Cl_3]$, the magnetic susceptibility is similar to those of the compounds which show spin-glass behavior such as $[Ni([15]aneN_4)N_3]PF_6$. The magnetization curve shows hysteresis, which means a weak ferromagnetic interaction.

## Acknowledgements

We are grateful to Dr K. Katsumata and Z. Honda (RIKEN), Dr T. Takeuchi (Osaka Univ), and Professor K. Awaga (University of Tokyo) for collaboration and many enlightening discussions.

## References

[1] J.S. Miller(Ed.), Extended Linear Chain Compounds, vols. I–III, Plenum, New York/London, 1982.
[2] H. Bethe, Z. Physik 71 (1931) 205.
[3] L. Hulthen, Arkiv. Mat. Astron. Fysik 26A (1938) 11.
[4] C.N. Yang, C.P. Yang, Phys. Rev. 150 (1966) 321.
[5] R.B. Griffiths, Phys. Rev. 133 (1964) A768.
[6] J.C. Bonner, M.E. Fisher, Phys. Rev. 135 (1964) A640.
[7] P.W. Anderson, Phys. Rev. 86 (1952) 694.
[8] R. Kubo, Phys. Rev. 86 (1952) 929.
[9] J. des Cloizeaux, J.J. Pearson, Phys. Rev. 128 (1962) 2131.
[10] F.D.M. Haldane, Phys. Rev. Lett. 50 (1983) 1153.
[11] M.P. Nightingale, H.W.J. Blote, Phys. Rev. B33 (1986) 659.
[12] T. Sakai, M. Takahashi, Phys. Rev. B42 (1990) 1090.
[13] A. Meyer, A. Gleizes, J.-J. Girerd, M. Verdaguer, O. Kahn, Inorg. Chem. 21 (1982) 1729.
[14] J.P. Renard, M. Verdaguer, L.P. Regnault, W.A.C. Erkelens, J.R. Mignod, W.G. Stirling, Europhys. Lett. 3 (1987) 945.
[15] G.E. Granroth, M.W. Meisel, M. Chaparala, Th. Jolicoeur, B.H. Ward, D.R. Talham, Phys. Rev. Lett. 77 (1996) 1616.
[16] S. Ma, C. Broholm, D.H. Reich, B.J. Sternlieb, R.W. Erwin, Phys. Rev. Lett. 69 (1992) 357.
[17] K. Katsumata, H. Hori, T. Takeuchi, M. Date, A. Yamagishi, J.P. Renard, Phys. Rev. Lett. 63 (1989) 86.
[18] T. Yosida, M. Fukui, J. Phys. Soc. Jpn. 61 (1992) 2304.
[19] J.P. Renard, M. Verdaguer, L.P. Renault, W.A.C. Erkelens, J.R. Mignod, J. Ribas, W.G. Stirling, C. Vettier, J. Appl. Phys. 63 (1988) 3538.
[20] T. Takeuchi, M. Ono, H. Hori, T. Yosida, A. Yamagishi, M. Date, J. Phys. Soc. Jpn. 61 (1992) 3255.
[21] M. Yamashita, Z. Honda, K. Katsumata, unpublished data.
[22] V. Gadet, M. Verdaguer, V. Briois, A. Gleizes, J.-P. Renard, P. Beauvillain, C. Chappert, T. Goto, K. Le Dang, P. Veillet, Phys. Rev. B44 (1991) 705.
[23] L.-K. Chou, K.A. Abboud, D.R. Talham, W.W. Kim, M.W. Meisel, Physica B 194-196 (1994) 311.
[24] T. Kobayashi, A. Kohda, K. Amaya, M. Ito, H. Deguchi, K. Takeda, T. Asana, Y. Ajiro, M. Mekata, J. Phys. Soc. Jpn. 63 (1994) 1961.
[25] J.-P. Renard, L.P. Renault, M. Verdaguer, J. Phys. 49 (1988) C8.
[26] T. Takeuchi, H. Hori, T. Yosida, A. Yamagishi, K. Katsumata, J.-P. Renard, V. Gadet, M. Verdaguer, M. Date, J. Phys. Soc. Jpn. 61 (1992) 3262.
[27] M. Yamashita, K. Inoue, T. Ohishi, H. Miyamae, T. Takeuchi, T. Yosida, Synth. Met. 71 (1995) 1961.
[28] T. Takeuchi, T. Yosida, K. Inoue, M. Yamashita, T. Kumada, K. Kindo, S. Merah, M. Verdaguer, J.-P. Renard, J. Mag. Mag. Mat. 140 (1995) 1633.
[29] Z. Honda, K. Katsumata, H.A. Katori, K. Yamada, T. Ohishi, T. Manabe, M. Yamashita, J. Phys. Condens. Matter 9 (1997) L83.
[30] M. Yamashita, H. Shimizu, K. Sakoyama, T. Manabe, T. Otsuka, K. Awaga, Synth. Met. 103 (1999) 2162.

[31] M. Monfort, J. Ribas, X. Solans, M.F. Bardia, Inorg. Chem. 35 (1996) 7633.
[32] Z. Honda, H. Asakawa, K. Katsumata, Phys. Rev. Lett. 81 (1998) 2566.
[33] A. Escuer, R. Vincente, J. Ribas, M.S.E. Fallah, X. Solans, M.F. Bardia, Inorg. Chem. 32 (1993) 3727.
[34] A. Escuer, R. Vincente, M.S.E. Fallah, J. Ribas, X. Solans, M.F.-Bardia, J. Chem. Soc. Dalton Trans. (1993) 2975.
[35] M. Yamashita, K. Inoue, T. Ohishi, T. Takeuchi, T. Yosida, W. Mori, Mol. Cryst. Liq. Cryst. 274 (1995) 25.
[36] T. Manabe, M. Yamashita, T. Ohishi, T. Takeuchi, T. Yosida, Y. Yu, Z. Honda, K. Katsumata, Synth. Met. 85 (1997) 1717.
[37] A. Escuer, R. Vicente, X. Solans, J. Chem. Soc. Dalton Trans. (1997) 531.
[38] H. Kikuchi, Y. Ajiro, N. Mori, T. Goto, H. Aruga, Solid State Comm. 76 (1990) 999.
[39] H. Mutka, J.L. Soubeyroux, G. Bourleax, P. Colombet, Phys. Rev. B39 (1989) 4820.
[40] A.J. Cox, J.G. Louderbaek, L.A. Mloomfield, Phys. Rev. Lett. 71 (1993) 923.
[41] Y. Yu, Z. Honda, K. Katsumata, T. Ohishi, T. Manabe, M. Yamashita, Mol. Cryst. Liq. Cryst. 286 (1996) 121.
[42] H.A. Goodwin, R.N. Sylva, Aust. J. Chem. 20 (1967) 629.
[43] S.P. Perlepes, et al., Inorg. Chem. 30 (1991) 1665.
[44] M. Yamashita, et al., unpublished data.